A Search for Close Binaries in the ρ Ophiuchus Star-Forming Region

M. Barsony[1,2]
Jet Propulsion Laboratory, Mail Stop 169-327
4800 Oak Grove Drive, Pasadena, CA 91109
`fun@uhuru.jpl.nasa.gov`

C. Koresko[2]
Michelson Science Center
California Institute of Technology
1201 E. California Blvd., Pasadena CA 91125
`koresko@fitzgerald.jpl.nasa.gov`
and

K. Matthews
Caltech Optical Observatory
California Institute of Technology
Pasadena, CA 91125
`kym@caltech.edu`

ABSTRACT

We have carried out a new, near-infrared speckle imaging survey of 19 members of the young stellar population in the nearby (d=140 pc), ρ Ophiuchi cloud core. Results for four binary and one newly discovered triple system are reported. Data for all known multiple systems among the pre-main-sequence population of ρ Oph are tabulated. We define a *restricted binary fraction* $F_{b,r}$ and a *restricted companion fraction* $F_{c,r}$ as counting only those systems most detectable in the present and previous high-resolution near-infrared imaging surveys, having separations between $0.''1$ and $\sim 1.''1$ and K-band magnitude differences $\Delta K < 3$. Analysis of all the available multiplicity data results in updated values of $F_{b,r} = 24\% \pm 11\%$ and $F_{c,r} = 24\% \pm 11\%$ for the Ophiuchus pre-main-sequence population. These values are consistent with the values in the Taurus star-forming region, and $F_{c,r}$ is in excess by a factor of 2 relative to the Main Sequence at the 1 σ level.

Subject headings: binaries:close — infrared:stars — stars:pre-main sequence — techniques: high angular resolution

1. Introduction

The formation of binary and multiple stars is a natural consequence of present-day star formation, yet many basic questions regarding this process remain unanswered. What is the frequency of multiple systems in the nearest star-forming regions to Earth? What is the distribution of source sepa-

---

[1] and Space Science Institute, 3100 Marine Street, Suite A353, Boulder, CO 80303-1058

[2] Based on observations obtained at the Hale telescope, Palomar Observatory, as part of a continuing collaboration between the California Institute of Technology, NASA/JPL, and Cornell University.

rations among pre-main-sequence binaries? Does this distribution evolve with time as the stars join the Main Sequence field population? Does the binary separation distribution vary with disk parameters, and if so, how? Do close binaries affect the appearance of each individual disk, and if so, how ?

It has been suggested that the binary frequency among T-Tauri stars in Taurus and Ophiuchus is higher than among the nearby solar-like stars in a restricted separation range (Ghez, Neugebauer, & Matthews 1993; Leinert et al. 1993). This separation range is $0''.1$-$1''.8$, corresponding to projected linear separations of 14-250 AU at an assumed 140 pc distance to the Taurus and Ophiuchus star-formation regions. Subsequent investigations of this claim have found conflicting, or at least, ambiguous, results for different star-forming regions (e.g., Prosser et al. 1994; Simon et al. 1995; Beck, Simon, & Close 2003). In Ophiuchus, in particular, there have been too few known multiple systems, with too few systems searched with comparable techniques, to have enough statistics for comparison with the main-sequence population and with other star-forming regions.

One problem, until recently, had simply been that too few actual cloud members were known in ρ Oph (e.g., Wilking, Lada, & Young 1989). This is due to the high overall extinction towards the ρ Oph cloud core, in contrast to the much lower extinction towards members of the young stellar population in Taurus. The advent of recent satellite data identifying young stellar objects (YSOs) in ρ Oph from the X-ray (Casanova et al. 1995; Grosso et al. 2000; Imanishi, Koyama, & Tsuboi 2002) and the mid-infrared (Bontemps et al. 2001) wavelength regions has significantly increased the known number of cloud members. Large-area, magnitude-limited, near-infrared surveys of ρ Oph have recently become available (Barsony et al. 1997; 2MASS[3]). The vast majority ($\sim$ 95%) of the near-infrared sources are background objects. However, positional cross-correlation of the near-infrared sources with lists of known cloud members, arrived at through observations at X-ray, mid-infrared, or optical wavelengths, allows the identification of suitable targets that meet the joint criteria of cloud membership and being bright enough at K-band (2.2 μm) for speckle imaging.

Once cloud members have been identified, a survey for multiplicity should ideally be undertaken such that all targets are searched using uniform criteria. The lack of consistency of previous surveys has made it difficult to draw firm conclusions regarding the binary fraction in ρ Oph. Previous multiplicity surveys in ρ Oph have used a variety of search techniques, including spectroscopy and imaging, at different wavelengths (either near-infrared or optical), with different sensitivities, valid over different separation ranges. One would ideally use a single technique, with the same sensitivity for all targets searched, obviating the need for various corrections due to lack of uniform data (e.g. Duchene 1999).

The largest number of binary identifications among pre-main-sequence members of the Taurus-Auriga dark clouds were found by high-resolution near-infrared imaging techniques (Ghez, Neugebauer, & Matthews 1993; Leinert et al. 1993; Simon et al. 1995). In practice, these techniques require relatively bright targets ($K \leq 8.5$ on a 5-meter aperture telescope for speckle imaging).

We have undertaken a new near-infrared speckle imaging survey of *bona fide* ρ Oph cloud members at the Hale 5-meter telescope. Since the *Chandra*, *ROSAT*, and *ISOCAM* surveys covered rather limited areas, of order $35' \times 35'$, containing rather few bright K-band targets that had not previously been searched, we supplemented our target list with bright K-band sources that are optically identified cloud members, either from large-area ground-based Hα surveys (Struve & Rudjkobing 1949; Dolidze & Arakelyan 1959; Wilking, Schwartz, & Blackwell 1987) or via optical follow-up imaging of *Einstein*-identified cloud members (Bouvier & Appenzeller 1992).

We report our target list, observing procedures, and data reduction methods in §2. The results of this speckle survey are presented in §3. In the Discussion (§4), we have collected published data on 49 separate multiple systems in Table 3, and the data on all systems found to be singles via high-resolution near-infrared techniques in Table 4, in order to be able to draw valid, statistically significant conclusions about the binary separation

---

[3] 2 Micron All Sky Survey Second Incremental Release Point Source Catalog, available at `http://irsa.ipac.caltech.edu`

distribution and the binary fraction in ρ Oph. We summarize our findings in §5.

2. Observations and Data Reduction

Speckle observations of the 19 pre-main sequence stars in the sample were made in the near-infrared K band on 24-25 May 2002 at the 5 m Hale telescope on Palomar Mountain. An external optical system (re-imager) magnified the telescope platescale to produce a pixel size of $0''.034 \pm 0''.001$, sufficient to Nyquist sample the $0''.1$ diffraction limit of the telescope (Weinberger 1998). The detector was D-78, a camera at the Cassegrain focus which was equippped with a 256×256 pixel InSb array, of which we used the central 64×64 pixels, giving a field-of-view of $2''.2$. The orientation accuracy of the detector is 0.5°. The seeing was typically $0''.75$ FWHM. The presence of thin cirrus prevented us from obtaining absolute photometry.

The observing procedure was typical for speckle interferometry, with the exception that the chopping secondary was used to switch rapidly between the position of the science target and the blank sky $30''$ away. Briefly, the data consisted of series of 560 frames with 0.1 second exposure times–fast enough to “freeze” the atmospheric seeing and preserve diffraction-limited image information. Sky exposures were interleaved with the exposures on the science target. In total, each series contained 490 frames on the target and 60 on the sky position, with the remaining 10 being rejected while the secondary's position was changing. At least 8 such series were obtained on each science target, along with a similar number on an unresolved reference star. The reference-star series were interleaved with the target-star series to reduce sensitivity to seeing and focus changes. A log of the observations is given in Table 1.

Reduction of the data consisted of the usual flatfielding and sky-subtraction of the raw frames, followed by computation of the Fourier power spectrum and bispectrum (Lohman, Wiegelt, & Wirnitzer 1983) averaged for the on-source frames in each series. The power spectrum of the calibrated sky frames in the series was subtracted from that of the on-source frames, and the Fourier phase for the series was reconstructed from the bispectrum using the recursive technique. The results for the science target series were calibrated pairwise with the results for the reference-star series to remove the distortions due to the atmosphere and the telescope. The calibration consisted of simple division of the sky-subtracted Fourier power spectra and subtraction of the reconstructed Fourier phases. The calibrated Fourier transform data were then averaged over the series for each science target. Finally, the calibrated Fourier data were apodized to approximately diffraction-limited resolution and Fourier transformed to recover a calibrated high-resolution image.

Basic parameters (the separation, position angle, and brightness relative to the primary) for the companions in the detected binary and triple systems were derived by fitting models to the calibrated Fourier data. Parameter uncertainties were estimated by fitting simulated data representing binaries with parameters close to the observed values. The simulated data were created by calibrating reference star files against each other to produce Fourier power spectra and phases for point sources. Their noise should be very similar to that for the calibrated science target data. The modulations corresponding to double-stars were then impressed onto the point-source power spectra by multiplying them by the power spectra of model doubles, and onto the point-source phases by adding the phases of the model doubles. In total, 23 independent simulated Fourier transforms were constructed for each real double detected in our survey. The results of fitting these simulated data could then be compared directly to the true model parameter values. The values we quote are the root-mean-squared scatter among the fits to the simulated datasets. We found that the separation error was independent of the separation and close to $0''.03$ for all doubles, while the position angle error ranged from $\sim 0.1^\circ$ for separation $0''.7$ to 20° for the marginally-resolved double with separation $0''.04$. The brightness ratio errors (with the ratio defined as the brightness of the fainter star divided by that of the brighter one) are ~ 0.03 for the fully-resolved doubles and 0.15 for the marginally-resolved double. These error estimates do not include the uncertainties in the image scale and orientation of the detector. Further, there is a 180° ambiguity in the position angle of the marginally-resolved double in the ROXs

47A hierarchical triple system.

3. Results

Of the 19 target objects for which we acquired near-infrared speckle data, five were resolved into multiple systems. Figures 1-5 show images related to each multiple system, with three frames plotted for each of the five panels. The leftmost panels represent the calibrated power spectra and the middle panels represent the Fourier phases, both plotted over spatial scales ranging from $1.1''$at the circles' centers, corresponding to approximately half the field-of-view of the portion of the detector that was used, to the diffraction limit of $0''.1$, at the circles' outer peripheries. The rightmost frame in each panel shows the final reconstructed image for each target object. Only one system, the ROXs 47A triple system, is a newly reported multiple (see Table 2).

In Table 2 we present the parameters of the systems shown in Figures 1-5. Column 1 lists the target's name, column 2, the component separations in arcseconds, column 3, the position angle, E of N, relative to the brighter object at K, and the last column lists the flux ratio between the components at K. For reference, we also tabulate previously reported binary parameters, when available, in Table 2.

Comparison with the previously published data for four systems in Table 2 shows no discernible change in separations and position angles for the ROXs 2, IRS 2, and ROXs 29 binary systems. There is quite a large change in the ROXs 42C hierarchical triple system, however. Between 8 July 1990 and 24 May 2002, the projected source separation increased by $0''.12$ (corresponding to 17 AU at a distance of 140 pc), whilst the position angle has advanced by 18°.

4. Discussion

4.1. Distribution of Binary Separations

The distribution of binary separations is of interest to identify any possible evolution of this quantity with age when compared with Main Sequence stars, as well as to compare this distribution among different star-forming environments. The original motivation for examining the pre-main-sequence distribution of binary separations was to test the hypothesis that the apparent excess of pre-main-sequence multiple systems observed in Taurus and Sco-Oph, reflects a distribution in the pre-main-sequence phase which is more strongly peaked in the range of separations to which the surveys are most sensitive ($\sim 0''.1 \leq a \leq 1''.8$), rather than a true excess of multiples. In this scenario, there would be an evolution of the shape of the the distribution of binary separations with time, with the distribution becoming flatter by the time the stars reach the Main Sequence (Ghez et al. 1993).

In order to have a statistically significant sample for the determination of the distribution of binary separations among the young stellar population in ρ Oph, we have compiled a list of all the multiple sources so far identified in the literature, in addition to the multiple systems identified in the study reported here. This compilation is presented in Table 3. The first column of Table 3 lists each young stellar object's name, with some common alternate names for the object listed in the last column. Note that the designation ROX refers to "Rho Oph X-ray" source as detected by the *Einstein* Observatory (Montmerle *et al.* 1983), whereas ROXs refers to an optically detected object that falls within the rather large *Einstein* X-ray source error circle. This distinction is important, because in some cases more than one optical counterpart is associated with a single *Einstein* source (Bouvier & Appenzeller 1992).

Since, unfortunately, it is not unusual for a single source to have a dozen or more names in ρ Oph, for ease of identification and for reference, coordinates are necessary. We have therefore included J2000 coordinates, good to ± $0''.2$, from the 2MASS database (unless otherwise indicated) for each object in the second and third columns of Table 3. The fourth column of Table 3 indicates the type of multiplicity: whether the system is binary, spectroscopic binary, triple, or quadruple. Columns 5 and 6 list the component separations in arcseconds, and the position angle between the components, measured East of North, from the brighter source at K, respectively. Column 7 lists the reference from which the multiplicity data were gleaned, with the first listed reference being the one from which the data in columns 5 & 6 are taken. Finally, in addition to alternate common names for the given target, comments are also included in the last column of Table 3.

Among the 49 independent multiple systems listed in Table 3, there are 62 separations, which are plotted in the histogram of Figure 6. This represents an eight-fold increase in the number of separations available for study of the pre-main-sequence population in ρ Oph since the last such published histogram (e.g., in Simon et al. 1995). The data in Figure 6 are binned in intervals of log P, as in previous authors' works (Duquennoy & Mayor 1991; Simon et al. 1995). The overplotted curve is the separation distribution based on the period distribution for main-sequence Solar-type field stars (Duquennoy & Mayor 1991). The conversion from a period to a separation distribution uses the same assumptions as previous authors, i.e., two 0.5 $M_{\odot}$ stars in a circular orbit at 140 pc distance (Simon et al. 1995). The vertical scale of the Main Sequence distribution is chosen to correspond to the same integrated number of sources as went into the histogram (62).

We note that this sample is reasonably complete over the $\sim 0''.1 \leq a \leq\sim 2''$ projected separation interval, but may be seriously incomplete at the closest separations (where spectroscopic searches are necessary) and at the larger ($\geq 10''$) separations, where few systematic searches have been undertaken, and where contamination by background objects becomes an issue.

There are not yet enough individual components of the multiple systems listed in Table 3 that have classifications available as to whether they are WTTS (weak-lined T-Tauri stars), lacking accretion disks, or CTTS (classical T-Tauri stars), with accretion disks, to draw meaningful conclusions from the comparison of the WTTS vs. CTTS binary separation distributions. Such a comparison would be interesting for the study of the effects of binarity on disk evolution. In this context, we note that a recent *HST* spectroscopic study of a sample of 20 close ($\leq 1''$) binaries in Taurus found that 4 (20%) turn out to be in mixed CTTS/WTTS pairs (Hartigan & Kenyon 2003). Furthermore, there is a strong selection effect against finding spectroscopic binaries among the CTTS, i.e., against finding CTTS at the closest separations, since the veiling and emission lines characteristic of CTTS can easily overwhelm the photospheric absorption lines that are generally used to find spectroscopic binaries. With these caveats, however, hopefully, the individual components of the multiple systems in Table 3 will be characterized in the near future, and the samples will become large enough to allow just such a comparison.

4.2. Binarity and Multiplicity Fraction of the ρ Oph Pre-Main-Sequence Population

An accurate determination of the multiplicity fraction of the young embedded population in ρ Ophiuchus presumes, first of all, that our search list is restricted to *bona fide* association members (excluding foreground or background objects). In practice, this means that each target object have one or more indicator of YSO (young stellar object) status, such as bright X-ray emission, broad Hα equivalent width, photospheric Li absorption, associated nebulosity, high percentage optical polarization, infrared excess, and/or a distance determination placing it at the cloud's distance of $\sim 140 \pm 20$ pc.

A second requirement for an accurate determination of the multiplicity is knowledge of the number of systems that have been searched for multiplicity by various authors, but found to be single. We want the search sensitivities to be as uniform as possible. Therefore, we restrict this analysis to objects searched for multiplicity with near-infrared techniques that are generally sensitive to source separations $0''.1 \leq r \leq\sim 1.1''$, and $\Delta K \leq 3$ mag. These joint criteria have the added benefit of effectively excluding background objects that may be chance projections towards the same line-of-sight as the target objects.

In Table 4, therefore, we list all of the target objects searched for multiplicity by searches which would have been sensitive to detecting binaries with source separations in the range $0''.1 \leq r \leq\sim 1.1''$, and with component magnitude differences, $\Delta K \leq 3$ mag. These surveys used various techniques, such as speckle observations, as reported here and elsewhere (Ghez et al. 1993, Ageorges et al. 1997), lunar occultation measurements (Simon et al. 1995), and shift-and-add imaging data (Costa et al. 2000, Haisch et al. 2002). In Table 4, each target object's name is listed in the first column, its J2000 coordinates, from the 2MASS Second Incremental Release Point Source Catalog, are listed in the second and third columns, and the authors who have searched each target for multiplicity and found it to be single, are listed in the last column. In constructing the Table, we were careful not to count the same target object multiple times, even when referred to by different names by the different surveys.

Comparison of the data presented in Tables 3 & 4 for the ρ Oph cloud core with previous work on ρ Oph, other star-forming regions, and the Main Sequence, requires determination of the *binary fraction*, $F_b = \frac{B+T+Q}{S+B+T+Q}$, and the *companion star fraction*, $F_c = \frac{B+2T+3Q}{S+B+T+Q}$, where S is the number of single stars, B is the number of binary systems, T, the number of triple systems, and Q, the number of quadruple systems in the survey sample. These definitions assume that there is no restriction on magnitude differences between companions, or on separations between companions, an assumption that is clearly unattainable in practice. The quantity that one can measure is a *restricted binary fraction*, which is the binary fraction restricted to a stated magnitude difference between primaries and their secondaries, and in a given (physical, not angular) separation range. Hopefully, the stated restriction guarantees a *complete* sample, *i.e.,* that all binaries within the given separation and magnitude difference ranges would be detected by the given survey. Such a complete sample may be defined for a single, given survey, but cannot be determined *a posteriori*, when comparing datasets published by various authors. The best we can do is to choose restrictions which are the most likely to result in a complete sample over all the published studies.

Given all these caveats, our restricted sample from Tables 3 & 4 will encompass $\Delta K \sim 3$ and $0''.1 \leq \Delta\Theta \leq 1.1''$ for the ρ Oph cloud core. This sample is restricted to targets that were searched for multiplicity via high-resolution, near-infrared techniques *only* (e.g., by any of the six surveys of Ageorges et al. 1997, Costa et al. 2000, Ghez et al. 1993, Haisch et al. 2002, Simon et al. 1995, or this work). If we restrict our attention to the sub-sample of Table 3 searched for multiplicity by only these six surveys (32 of the 49 systems listed), then among this sub-sample there are 19 systems with at least one separation in the $0''.1 \leq \Delta\Theta \leq 1.1''$ range. Of the 32 multiple systems listed in Table 3 that were surveyed by the above-listed six surveys, there remain 13 systems with no separations in the restricted range. In addition, there are 48 distinct targets searched by these six surveys, which were found to be single (listed in Table 4). Thus, the *restricted binary fraction* is 19/(19+13+48), or 24% ± 11%. We note parenthetically that when a binary is found in this restricted $0''.1 \leq \Delta\Theta \leq 1.1''$ separation range, if it is part of a wider-separation triple or quadruple, we still consider the larger multiple system as a single target for counting purposes. Were we to count targets that are separated by $\geq 1.1''$ as individual targets for counting purposes, then we would get a lower value for the restricted binary fraction for ρ Oph. We therefore adopt the value of 24% ± 11% (19/(32+48)) as the *restricted binary fraction*, $F_{b,r}$, for the ρ Ophiuchi pre-main-sequence population in the $\sim 0''.1$–$\sim 1.1''$, $\Delta K \leq 3$ range.

Ghez et al. (1993) define their *complete sample* by the restrictions $\Delta K \leq 2$, $0''.1 \leq \Theta \leq 1''.8$ for Taurus and $\Delta K \leq 2$, $0''.1 \leq \Theta \leq 1''.6$ for Sco-Oph, since they assumed distances of 140 pc and 160 pc to Taurus and Ophiuchus, respectively, and the restriction on angular separation was meant as a restriction on true, projected, *physical* separations, corresponding to 16–252 AU in that study. The restricted binary star frequency among Oph-Sco targets, with the restrictions as defined by by Ghez et al. (1993) for Sco-Oph was 29% ± 12% from a sample of 21 targets. The restricted binary star fraction for this same set of constraints for Taurus was found to be 37% ± 9% from the 43 targets in their complete sample. Our newly derived value of 24% ± 11% from 80 Ophiuchus-only targets, restricted to a somewhat smaller physical separation range, but to a similar magnitude difference range between primaries and secondaries, is consistent, within the errors, with the restricted binary star frequency among the pre-main-sequence populations of Ophiuchus and Taurus being identical.

In a related study of X-ray selected T-Tauri stars in the Sco-Cen OB Association, which is at the same distance as the Ophiuchus cloud core, Köhler et al. (2000) used both near-infrared speckle and near-infrared direct imaging techniques in order achieve completeness limits for companions in the $0''.13 \leq a \leq 6''$and $\Delta K \leq 2.5$ mag ranges. They found 27 binaries and 2 triples from 88 targets, corresponding to 33% ± 11% for their restricted binary fraction, $F_{b,r} = (27 + 2)/88$), and 35% ± 11% for their restricted companion fraction, $F_{c,r} = (27 + 2 \times 2)/88$), after correcting for contamination by background objects and for X-ray selection bias. Although at first glance the restricted binary star frequency among the Sco-Cen and Ophiuchus samples is consistent with being identical within the errors, one must bear in mind that the separation range of $2'' \leq a \leq 6''$ was not sampled in Ophiuchus, whereas it was sampled in Sco-Cen.

We note that the physical separation range to which our discussion of the Ophiuchus and Taurus samples was restricted, would correspond to an angular separation range of $0''.03 \leq a \leq 0.37''$ at the distance to the Orion star-forming region. This angular separation range, although accessible with the largest (10-meter diameter) ground-based telescopes equipped with adaptive optics, has not yet been explored towards Orion (Beck et al. 2003; Simon et al. 1999). Therefore, at present, no direct comparison can be made between the restricted binary fractions in ρ Oph and Taurus, on the one hand, and Orion, on the other.

Comparison of the ρ Oph multiplicity fraction with that of the Main Sequence requires calculation of the *companion star fraction*, F_c, in this separation range. For the same restrictions ($\sim 0''.1$–$\sim 1.1''$, $\Delta K \leq 3$), as above, the restricted companion star fraction derived from the data presented in Tables 3 & 4, is 24% ± 11% for ρ Oph. This fraction is arrived at by counting three triples, V853, ROXs 42C, and ROXs 47A, from Table 3 as binaries, since the restriction on angular separations excludes some of the multiple components that are detected in these systems. The Main Sequence *companion star fraction* in the projected physical separation range, 16-252 AU, (corresponding to angular separations $0''.1 \leq \Theta \leq 1''.8$ at an assumed 140 pc distance to ρ Oph) is 16% ± 3% for stars in the $0.8\ \mathrm{M}\odot \leq M \leq 1.3\ \mathrm{M}_\odot$ mass range (Duquennoy & Mayor 1991), and 12% ± 4% for lower mass M dwarfs (Fischer & Marcy 1992). For purposes of comparison with the Main Sequence results, it must be borne in mind that the restricted companion star fraction derived for ρ Oph above is, a strict *lower* limit in the sense that we imposed an additional constraint, that of $\Delta K \leq 3$ on our sample, whereas no component flux ratio limits were imposed on the samples used to derive the Main Sequence restricted companion fractions. An over-abundance of multiple systems among the pre-main-sequence population of Ophiuchus relative to the Main Sequence over this restricted separation range is not yet a statistically significant (3 σ) result, however.

Future multiplicity surveys of the ρ Oph pre-main-sequence population at larger component separations, when combined with the data presented here, would decide the question of whether we are observing a true over-abundance of multiple systems among recently formed stars relative to the Main Sequence, or if we are witnessing the evolution of binary separations with time.

4.3. IRS 43, IRS 44, and IRS 51

As alluded to in the previous section, often several sets of authors have searched the same target for multiplicity (viz., Table 4). In general, search results reported by different sets of authors, but obtained with techniques sensitive to similar magnitude differences and to similar size-scales, agree well. However, there are three objects, IRS 43, IRS 44, and IRS 51, for which results amongst different authors, and even among the same authors, give conflicting or confusing results.

IRS 43 (YLW15A) is an unusual object in ρ Oph, because it is by far the strongest X-ray source, exhibiting powerful X-ray flaring activity (Grosso et al. 1997; Montmerle et al. 2000; Tsuboi et al. 2000). A VLA 3.6cm radio map of IRS 43 resolved two sources: VLA 1, a resolved, thermal jet, and VLA 2, a point source, positionally coincident (to within ± $0''.2$) with the bright near-infrared source, IRS 43 (Girart, Rodriguez, & Curiel 2000). Ground-based, mid-infrared imaging at the Keck II telescope with JPL's MIRLIN camera found a $0''.51$, PA= 332.7° binary associated with IRS 43, similar in appearance to the double 3.6 cm source (Haisch *et al.* 2002). However, ground-based near-IR measurements detected only a single NIR source (to K<12), associated with VLA 2,the South-Eastern 10μm component (Simon et al. 1995; Costa et al. 2000). IRS 43 was reported as a single source with *NICMOS* imaging through the 1.1 μm and 1.6 μm filters (Allen *et al.* 2002), but "two point-like sources clearly showing the *NICMOS* diffraction pattern" are reported by Terebey *et al.* 2001, who reached a 2000:1 dynamic range using the 2.05 μm filter. Nevertheless, Terebey et al. (2001) classify IRS 43 as a single object, with no further information given.

IRS 44 (YLW 16A) is, similarly, not resolved by ground-based measurements (Simon et al. 1995; Costa et al. 2000; Haisch et al. 2002). Allen *et al.* (2002) detect two non-point sources, separated by $0''.5$ at PA=270° with a flux ratio of 1.5 at 1.1 μm and 1.1 at 1.6 μm in their *NICMOS* images of IRS 44. They interpret this as scattered light from possibly a star/disk/envelope system. Terebey *et al.* (2001), on the other hand, report the detection of two point sources, at a separation of $0''.27$ at P.A. = 81°, with the primary detected in all three (F160W, F187W, and F205W) *NICMOS* images, and the secondary detected only at the longest, 2.05 μm, wavelength.

IRS 51, although found to be a point source by Simon et al. (1995) and by Costa et al. (2000), was found to be extended in H, K, and L shift-and-add imaging by Haisch et al. (2002). Whereas the near-infrared images presented by Haisch et al. are consistent with a secondary at P.A. = 10° at $1''.5$ separation, the mid-infrared image of the same object, at similarly high angular resolution, consists of extended emission, with an emission "knot" at just $0''.7$ separation at P.A. = 15°. Clearly, the source of the extended near- and mid-infrared emission surrounding this object deserves further study.

5. Summary

- We have carried out a new, near-infrared, speckle imaging survey of 19 pre-main-sequence objects in ρ Ophiuchus, of which four are binary, and one is a newly discovered triple system.

- We have tabulated all the close binaries known in the ρ Oph cloud core, as well as all of the ρ Oph cloud members searched for multiplicity, but found to be single, by various high-angular resolution, near-infrared techniques.

- Synthesis of the multiplicity data presented here results in the determination of 24% ± 11% for the *restricted binary fraction* of the Ophiuchus pre-main-sequence population in the $\sim 0''.1$–$1.1''$, $\Delta K \leq 3$ range. This can be compared with the 37% ± 9% *restricted binary fraction* found in the Taurus pre-main-sequence population over a $\Delta K \leq 2$, $0''.1 \leq \Theta \leq 1''.8$ range. Future adaptive optics observations towards Orion with 10-meter aperture telescopes, which can sample the $0''.03 \leq 0.4''.0$ angular separation range, will allow a direct comparison with the *restricted binary fraction* in Orion in the projected physical separation range, 16AU-154 AU.

- The observed *restricted companion fraction* derived from the data presented here is also 24% ± 11% for ρ Oph in a range restricted to $\sim 0''.1$–$1.1''$separations, and to magnitude differences, $\Delta K \leq 3$. Due to the magnitude difference constraint imposed on the ρ Oph sample, 24% ± 11% represents a strict *lower limit* to the true *restricted companion fraction* of ρ Oph in this separation range. In the physical separation range of 16-252 AU, the *true restricted companion fraction* for the Main Sequence is 16% ± 3% for stars in the 0.8 $M_\odot \leq M \leq 1.3$ $M_\odot$ mass range (Duquennoy & Mayor 1991), and 12% ± 4% for lower mass, Main Sequence M dwarfs (Fischer & Marcy 1992).

- Larger surveys for companions among the ρ Oph association members are required to definitively establish (to 3σ) the over-abundance of the companion fraction relative to that of the Main Sequence. Surveys for multiples at large separations in the ρ Oph population, corrected for background contamination, will help improve the statistics. Synthesis of multiplicity data from future surveys at all separations will decide whether it's the multiplicity fraction or the binary separation distribution that evolves with time from the pre-main-sequence to the Main Sequence.

We would like to thank the Palomar Office and staff for their help, expertise, and professionalism in running the Palomar Observatory. This research has made use of NASA's Astrophysics Data System Bibliographic Services, the SIMBAD database, operated at CDS, Strasbourg, France, and of the NASA/IPAC Infrared Science Archive, which is operated by the Jet Propulsion Laboratory, California Institute of Technology, under contract with the National Aeronautics and Space Administration. MB would especially like to acknowlege NSF grant AST-0206146 for making her contributions to this work possible. Additional support for this work was provided by the National Aeronautics and Space Administrations through Chandra Award Number AR1-2005A and AR1-2005B issued by the Chandra X-Ray Observatory Center, which is operated by the Smithsonian Astrophysical Observatory for and on behalf of NASA under contract NAS8-39073.

REFERENCES

Ageorges, N., Eckart, A., Monin, J.-L., & Ménard, F. 1997, A& A, 326, 632

Aitken, R.G. 1932, New General Catalogue of Double Stars within 120 degrees of the North Pole, Carnegie Institution of Washington: Washington, D.C. (Publication No. 417)

Allen, L.E., Myers, P.C., DiFrancesco, J., Mathieu, R., Chen, H., & Young, E. 2002, ApJ, 566, 993

Aspin, C., Puxley, P.J., Hawarden, T.G., Paterson, M.J., & Pickup, D.A. 1997, MNRAS, 284, 257

Barsony, M., Burton, M.G., Russell, A.P.G., Carlstrom, J.E., & Garden, R. 1989, ApJ, 346, L93

Barsony, M., Kenyon, S.J., Lada, E.A., & Teuben, P.J. 1997, ApJS, 112, 109

Beck, T., Simon, M., & Close, L.M. 2003, ApJ, 583, 358

Bontemps, S., André, P., Kaas, A.A., Nordh, L., Olofsson, G., Huldtgren, M., Abergel, A., Blommaert, J., Boulanger, F., Burgdorf, M., Cesarsky, C.J., Cesarsky, D., Copet, E., Davies, J., Falgarone, E., Lagache, G., Montmerle, T., Pérault, M., Persi, P., Prusti, T., Puget, J.L., & Sibille, F. 2001, A& A, 372, 173

Bouvier, J. & Appenzeller, I. 1992, A& AS, 92, 481

Casanova, S., Montmerle, T., Feigelson, E.D., & André, Ph. 1995, ApJ, 439, 752

Chelli, A., Cruz-Gonzalez, I., Zinnecker, H., Carrasco, L., & Perrier, C. 1988, A& A, 207, 46

Costa, A., Jessop, N.E., Yun, J.L., Santos, C., Ward-Thompson, D., & Casali, M.M. 2000 in *Birth and Evolution of Binary Stars*, Poster Proceedings of IAU Symp. No. 200, eds. B. Reipurth & H. Zinnecker, p. 48

Dolidze, M.V. & Arakelyan, M.A. 1959, AZh, 36, 444

Duchene, G., 1999, A& A, 341, 547

Duquennoy, A. & Mayor, M. 1991, A& A, 248, 485

Fischer, D.A. & Marcy, G.W. 1992, ApJ, 396, 178

Geoffray, H. & Monin, J.-L. 2001, A& A, 369, 239

Ghez, A., Neugebauer, G., & Matthews, K. 1993, AJ, 106, 2005

Girart, J.M., Rodriguez, L.F., & Curiel, S. 2000, ApJ, 544, 153

Grosso, N., Montmerle, T., Feigelson, E.D., André, P., Casanova, S., & Gregorio-Hetem, J. 1997, Nature, 387, 56

Grosso, N., Montmerle, T., Bontemps, S, André, P., & Feigelson, E.D., 2000, A& A, 359, 113

Haisch, K.E., Jr., Barsony, M., Greene, T.P., & Ressler, M.E. 2002, AJ, 124, 2841

Haffner, L.M. & Meyer, D.M. 1995, ApJ, 453, 450

Hartigan, P. & Kenyon, S.J. 2003, ApJ, in press

Imanishi, K., Koyama, K., & Tsuboi, Y. 2002, ApJ,, 557 747

Koresko, C. 2002, AJ, 124, 1082

Köhler, R., Kunkel, M., Leinert, C., & Zinnecker, H. 2000, A& A, 356, 541

Leinert, Ch., Zinnecker, H., Weitzel, N., Christou, J., Ridgway, S.T.., Jameson, R., Haas, M., & Lenzen, R. 1993, A& A, 278, 129

Mathieu, R., Walter, F.M., & Myers, P.C. 1989, AJ, 987

Lohmann, A.W., Weigelt, G., & Wirnitzer, B. 1983, ApOpt, 22, 4028

Montmerle, T., Koch-Miramond, L., Falgarone, E., & Grindlay, J.E. 1983, ApJ, 269, 182

Montmerle, T., Grosso, N., Tsuboi, Y., & Koyama, K. 2000, ApJ, 532, 1097

Prosser, C.F., Stauffer, J.R., Hartmann, L., Soderblom, D.R., Jones, B.F., Werner, M.F., McCaughrean, M.J. 1994, ApJ, 421, 517

Reipurth, B. & Zinnecker, H. 1993, A& A, 278, 81

Ressler, M.E. & Barsony, M. 2001, AJ, 121, 1098

Simon, M., Howell, R.R., Longmore, A.J., Wilking, B.A., Peterson, D.M., & Chen, W.-P. 1987, ApJ, 320, 344

Simon, M., Ghez, A., Leinert, Ch., Cassar, L., Chen, W.P., Howell, R.R., Jameson, R.F., Matthews, K., Neugebauer, G., & Richichi, A. 1995, ApJ, 443, 625

Simon, M., Close, L.M., & Beck, T.L. 1999, AJ, 117, 1375

Struve, O. & Rudjkobing, M. 1949, ApJ, 109, 92

Terebey, S., Van Buren, D., Hancock, T., Padgett, D.L., & Brundage, M. 2001, in *From Darkness to Light: Origin and Evolution of Young Stellar Clusters*, ASP Conf. Ser., Vol. 243, eds. T. Montmerle & Ph. André, p.243

Tsuboi, Y., Imanishi, K., Koyama, K, Grosso, N., & Montmerle, T. 2000, ApJ, 532, 1089

Weinberger, A. 1998, Ph.D. Thesis, Physics, California Institute of Technology

Wilking, B.A., Schwartz, R.D., & Blackwell, J.H. 1987, AJ, 94, 106

Wilking, B.A., Lada, C.J., & Young, E.T. 1989, ApJ, 340, 823

Zhang, Q., Wootten, A., Ho, P.T.P. 1997, ApJ, 475, 713

This 2-column preprint was prepared with the AAS LaTeX macros v5.0.

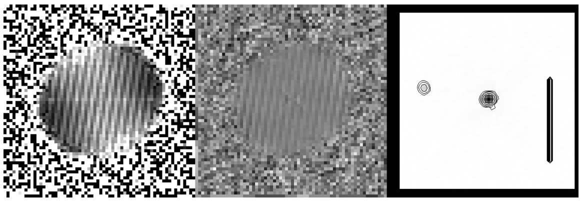

Fig. 1.— From left to right are shown the calibrated Fourier power spectrum, Fourier phases, and the reconstructed image for the newly discovered hierarchical triple system, ROXs 47A. The Fourier power spectra and phases exhibit a pattern of narrow stripes characteristic of a well-resolved binary. The superposed single broad stripe in the power spectrum signals the presence of the third, marginally-resolved star in the system. Careful comparison of the shapes of the stellar images in the reconstructed image reveals a slight extension in the primary along a direction perpendicular to the broad bar in the power spectrum. The simplest explanation for this is that the primary is itself a binary at $0''.04$ separation. The well-separated third component at P.A.= 80.8° is $0''.79$ away. The vertical scalebar's length is $1''$, and the image orientation has North up and East to the left.

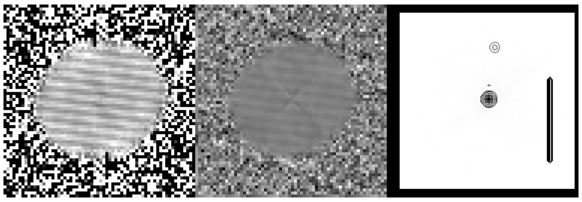

Fig. 2.— From left to right are shown the calibrated Fourier power spectrum, Fourier phases, and the reconstructed image for the ROXs 29 binary sytem. The image orientation has North up and East to the left. The vertical scalebar's length is 1″. The binary separation is 0″.63 at PA 353°, with a brightness ratio of 12.

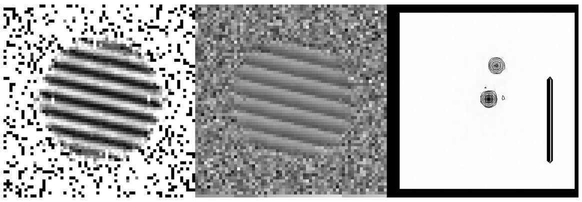

Fig. 3.— From left to right are shown the calibrated Fourier power spectrum, Fourier phases, and the reconstructed image for the ROXs 2 binary system. The image orientation has North up and East to the left. The vertical scalebar's length is 1″. The binary separation is 0″.42 at PA 347°, with a brightness ratio of 1.75.

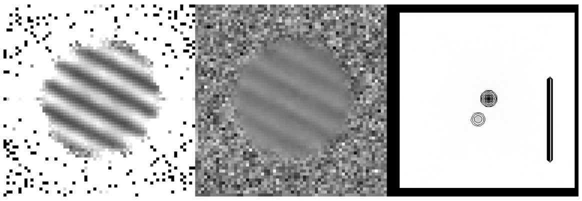

Fig. 4.— From left to right are shown the calibrated Fourier power spectrum, Fourier phases, and the reconstructed image for the ROXs 42C hierarchical triple system. The image orientation has North up and East to the left. The vertical scalebar's length is $1''$. The source separation is $0''.28$ at PA 153°, and the brightness ratio of the resolved components is 4.4. One of these components is itself a spectroscopic binary (Mathieu et al. 1989). This is the only system in which a significant change in the orbital parameters was observed. For comparison, the previously published binary separation was $0''.16$ at PA 135° (Ghez et al. 1993).

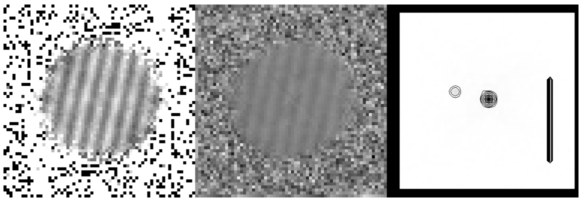

Fig. 5.— From left to right are shown the calibrated Fourier power spectrum, Fourier phases, and the reconstructed image for the IRS 2 binary system. The image orientation has North up and East to the left. The vertical scalebar's length is $1''$. The binary separation is $0''.42$ at PA 78°, with a brightness ratio of 8.

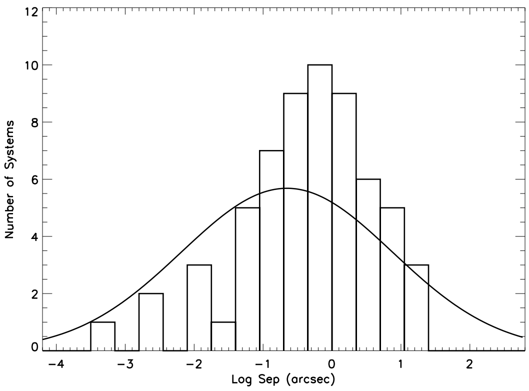

Fig. 6.— Distribution of the separations of the pairs in the binary and multiple systems of Table 3. The overplotted curve corresponds to the distribution of separations in Solar-type Main Sequence stars as measured by Duquennoy & Mayor (1991), and is scaled to correspond to the number of pre-main sequence systems plotted. The separations for the Main Sequence stars are computed according to the same assumptions as used by previous workers: a distance of 140 pc, stellar component masses of 0.5 $M_{\odot}$, and circular orbits.

TABLE 1
OBSERVING LOG

Target	Night	Series	RA (2000)	Dec (2000)
V852 Oph	24 May 2002	8	16 25 22.16	-24 30 13.7
ROXs 2	24 May 2002	8	16 25 24.37	-23 55 09.9
IRS2	24 May 2002	8	16 25 36.75	-24 15 42.1
ROXs 4 IRS10	24 May 2002	8	16 25 50.53	-24 39 14.3
ROXs 10A/DoAr24	24 May 2002	8	16 26 17.09	-24 20 21.4
ROXs 9A	24 May 2002	8	16 26 23.99	-25 47 16.1
ROXs 9B	24 May 2002	8	16 26 30.72	-25 43 39.8
ROXs 9C	24 May 2002	8	16 26 37.95	-25 45 12.8
GY292	24 May 2002	10	16 27 33.11	-24 41 15.1
ROXs 35A	24 May 2002	8	16 27 38.31	-23 57 32.9
WSB52/GY314	24 May 2002	8	16 27 39.43	-24 39 15.5
ROXs 29/SR 9	24 May 2002	8	16 27 40.28	-24 22 04.3
ROXs 40	24 May 2002	8	16 30 51.51	-24 11 34.0
WSB69A	25 May 2002	10	16 31 04.37	-24 04 33.3
WSB69b	25 May 2002	8	16 31 05.17	-24 04 40.3
ROXs 42C	24 May 2002	8	16 31 15.75	-24 34 02.2
ROXs 44	24 May 2002	8	16 31 33.45	-24 27 37.1
IRAS 16289-2457	24 May 2002	8	16 31 54.74	-25 03 23.8
ROXs 47A	24 May 2002	8	16 32 11.81	-24 40 21.3

TABLE 2
CHARACTERISTICS OF MULTIPLE SYSTEMS DETECTED IN THIS SURVEY

System	Separation (″)	P.A. (°)	Flux Ratio[1]	Ref.
ROXs 2	0.42 ± 0.03	347.1 ± 0.2	1.75 ± 0.1	This work
	0.41 ± 0.03	349 ± 1	2.58 ± 0.3	C00
IRS2	0.42 ± 0.03	77.6 ± 0.4	8.0 ± 2.5	This work
	0.44 ± 0.03	79 ± 4	7.58 ± 0.4 at H-band	C00
ROXs 29/SR 9/Elias 34	0.63 ± 0.03	353.3 ± 0.05	12 ± 5	This work
	0.59 ± 0.01	350 ± 1	11 ± 2; 13±2	G93
ROXs 42C[2]	0.28 ± 0.03	152.9 ± 0.5	4.4 ± 0.7	This work
	0.157 ± 0.003	135 ± 3	4.0 ± 0.34	G93
ROXs 47A	0.79 ± 0.03	80.8 ± 0.1	2.5 ±0.2	This work
ROXs 47A[3]	0.04 ± 0.03	107 ± 20	1.1 ±0.7	This work

[1] All flux ratios are at K-band, except where otherwise noted.

[2] This is a triple system, with one component consisting of a spectroscopic binary (Mathieu et al. 1989)

[3] Due to the extreme proximity of the components, there remains a 180° ambiguity in the position angle of the close binary in this hierarchical triple system.

REFERENCES.—C00=Costa et al. 2000; G93=Ghez et al. 1993

Table 3

Separations of Binary/Multiple Systems in Ophiuchus

Name	α(2000)	δ(2000)	System Type[1]	Sep'n. Arcsec	P.A. Deg[2]	Refs.[3]	Oth Alia
155203-2338	15 54 59.87	-23 47 18.2	B	0.80	229	G93	
WSB 3	16 18 49.61	-26 32 53.3	B	0.60	162	RZ93	
WSB 4	16 18 49.66	-26 10 06.2	B	2.84	128.5	K02,RZ93	IRC[4](RZ93)
WSB 11[5]	16 21 57.3	-22 38 16	B	0.50	N.A.	RZ93	
WSB 18	16 24 59.79	-24 56 00.3	T(Q?)	1.08	80.4	K02,RZ93	Faint 2MASS src. @ 10
WSB18A				0.100	339.55	K02,RZ93	Primary is double
WSB 19	16 25 02.13	-24 59 31.8	B	1.53	260.7	K02,RZ93	
WSB 20[5]	16 25 10.5	-23 19 14	B	1.0	23	GM01,RZ93	
ROX 1	16 25 19.28	-24 26 52.1	B	0.236	156	G93,A32	SR2, SAO 184375, Elias
HD 147889[5]	16 25 24.32	-24 27 56.6	B	4.09×10^{-4}	N.A.	HM95	SpB; Period=5d; SR1,
ROXs 2	16 25 24.37	-23 55 09.9	B	0.41	349	C00;This work	
IRS 2	16 25 36.75	-24 15 42.1	B	0.44+/-0.03	79+/-4	C00;This work	
ROXs 5	16 25 55.86	-23 55 10.1	B	0.13	130	A97	
WSB 26	16 26 18.40	-25 20 55.6	B	1.15	23.8	K02,RZ93	DoAr 23
WSB 28			B	5.1	358	RZ93	
WSB 28 Primary	16 26 20.99	-24 08 51.8					
WSB 28 Secondary	16 26 20.99	-24 08 46.7					
DoAr 24E	16 26 23.38	-24 20 59.7	B	2.05	148.6	K02,C00,A97,S95,C88	ROXs 10B, Elias 22, GS
Elias23+GY21			B	10.47	322.6	HBGR02	
Elias 23	16 26 24.06	-24 24 48.1				GSS32 is single (S95;T01;HBGR02)	S2,GSS32,GY23
GY 21	16 26 23.60	-24 24 39.4				GY21 is single (C00;HBGR02)	
VSSG 27	16 26 30.50	-24 22 57.1	B	1.22+/-0.03	68 +/-1	C00	GY51
S1	16 26 34.18	-24 23 28.2	B	0.020	110	S95	ROXs 14, GY70, GSS35
WSB 35[5]	16 26 34.8	-23 45 41	B	2.29	130.3	K02,RZ93	DoAr 26
GSS37	16 26 42.87	-24 20 29.8	B(T?)	1.44	67.0	K02,C00,RZ93	ROX 15, Elias 26;2MAS
VSS27	16 26 46.44	-24 12 00.0	B	0.59	104.6	A97,C00	ROXs 16, WSB38
WL 2			B	4.17	343	B89	
WL 2(A)	16 26 48.50	-24 28 38.7					
WL 2(B)	16 26 48.42	-24 28 34.7					
WL 18	16 26 48.99	-24 38 25.1	B	3.55	293	B89	
VSSG 3	16 26 49.25	-24 20 02.9	B	0.25+/-0.03	47 +/-1	C00	GY135; @24.5” is BKL
SR 24			T	6.00(5.093”)	60	S95;(2MASS)	WSB 42
SR 24A	16 26 58.52	-24 45 36.7				SR 24S	G93 found SR 24S to be
SR 24B	16 26 58.45	-24 45 31.7		0.197	84	S95;C00	SR 24N, DoAr 29
WL 1	16 27 04.12	-24 28 29.9	B	0.82	321.2	HBGR02;C00	
SR21			B	6.7 (6.33”)	175	S95;(2MASS)	Elias 30; VSSG23
SR 21A	16 27 10.28	-24 19 12.6					
SR 21B	16 27 10.33	-24 19 18.9					
ROXs 20A+ROXs 20B			B	10.0	126	BA92	
ROXs 20A	16 27 14.51	-24 51 33.4				Secondary	WSB45, HBC640
ROXs 20B	16 27 15.15	-24 51 38.8				Primary	WSB46, HBC641
WL20			T			RB01	
WL20W	16 27 15.69	-24 38 43.4		3.17	270	RB01	E-W sep'n.
WL20S	16 27 15.72	-24 38 45.6		2.26	173	RB01	S-W sep'n.
WL20E	16 27 15.89	-24 38 43.4		3.66	232	RB01	S-E sep'n.
SR 12+IRS42			T(?)			This work, BKLT97, 2MASS	
SR 12	16 27 19.52	-24 41 40.4	B	0.30+/-0.03	85	S95;C00	ROXs 21, IRS40, GY25
IRS42	16 27 21.48	-24 41 43.0		26.8	85.8	S95;C00 found IRS42 single	GY252
GY263+GY265			B(T?)	6.99	322	HBGR02;S95	YLW15A; CRBR85 is 3
GY263	16 27 26.63	-24 40 44.9					
IRS 43[6]	16 27 26.94	-24 40 50.				HBGR02;T01;C00;S95	GY265

TABLE 3—*Continued*

Name	α(2000)	δ(2000)	System Type^1	Sep'n. Arcsec	P.A. Deg^2	Refs.^{3}	
IRS 44+GY262			T(?)				
GY262	16 27 26.49	-24 39 23.0		23.21		T01	
IRS 44^6	16 27 28.01	-24 39 33.6	B	0.27	81	HBGR02;T01;C00;S95	YLW16A
WL 13	16 27 27.40	-24 31 16.6	B	0.46	356	C00	VSSG25; Elia
VSSG 17	16 27 30.17	-24 27 43.5	B	0.25+/-0.03	26 +/-6	C00	Elias 33/IRS4
DoAr32+DoAr33			T	48	170	BA92	
DoAr32	16 27 38.31	-23 57 32.9	B	10.06	332.1	A97	WSB51, ROX
DoAr33	16 27 39.00	-23 58 19.0					WSB53, ROX
SR9	16 27 40.28	-24 22 04.3	B	0.59	350	GM01,G93;This work	ROXs 29, Elia
VSSG 14	16 27 49.86	-24 25 40.5	B	0.101	89	S95	Elias 36; GY3
ROXs 31	16 27 52.07	-24 40 50.4	B	0.39	71.6	A97,S95,S87,C00	IRS 55/GY380
SR 20	16 28 32.68	-24 22 45.0	B	0.071	225	G93;S95	ROX 33, WSB
V853 Oph	16 28 45.29	-24 28 18.9	T	0.43	97	S95;G93;C00;GM01	SR 13, WSB6
V853 Oph A				0.013	96	S95	Primary resol
Haro1-14c+Haro1-14			B	12.9	122	RZ93	
Haro1-14c	16 31 04.37	-24 04 33.3					Primary
Haro1-14	16 31 05.17	-24 04 40.3					WSB69; Secon
ROX 42B	16 31 15.02	-24 32 43.7	B	0.056	89	S95	
ROXs 42C	16 31 15.75	-24 34 02.2	T	0.157	135	G93;This work+SpB M89	
ROXs 42C				0.00195		SpB P=35.95 days; M89	
ROXs 43			Q	4.67/4.80/4.3(4.39)	13.7/7/13	A97/S95/RZ93(2MASS)	A and B sepa
ROXs 43 A	16 31 20.12	-24 30 05.0		0.0028	N.A.	M89	SpB P=89.1 ±
ROXs 43 B	16 31 20.19	-24 30 00.7		0.016	89	S95	
WSB 71			B(T?)	3.56	35.0	K02;S95	Faint 2MASS
WSB 71A	16 31 30.88	-24 24 39.9					
WSB 71B	16 31 31.04	-24 24 37.0					
L1689 IRS5	16 31 52.12	-24 56 15.7	B	2.92	240.3	HBGR02	L1689 SNO2
ROXs 45E+ROXs 45F			B	15.0	75	BA92	
ROXs 45E	16 32 00.5	-25 30 29					DoAr49
ROXs 45F	16 32 01.6	-25 30 25					DoAr50
ROXs 47A	16 32 11.81	-24 40 21.3	T	0.813	80.5	This work	
ROXs 47Ab			B	0.046	107.9 or 287.9	This work	
HD 150193	16 40 17.93	-23 53 45.3	B(T?)	1.09	221.7	K02	Elias 49 (HAe

[1] B=Binary; SpB=Spectroscopic Binary; T=Triple; Q=Quadruple

[2] PAs are E of N, measured from the primary at K

[3] Separations and PAs listed are from the first reference

[4] IRC=Infrared Companion system

[5] Coordinates for WSB 11, WSB 20, & WSB 35 are from the SIMBAD database; these sources fell outside the 2MASS survey's areal coverage.

[6] See text for discussion of IRS 43, IRS 44, & IRS 51.

REFERENCES.—A97=Ageorges et al. 1997; A32=Aitken 1932; B89=Barsony *et al.* 1989; BKLT97=Barsony et al. 1997; BA92=Bouvier & Appenzeller 1992; C88=Chelli et al. 1988; C00=Costa et al. 2000; GM01=Geoffray & Monin 2001; G93=Ghez et al. 1993; HM95=Haffner & Meyer 1995; HBGR02=Haisch et al. 2002; K02=Koresko 2002 M89=Mathieu *et al.* 1989; RZ93=Reipurth & Zinnecker 1993; S95=Simon et al. 1995; T01=Terebey et al. 2001

Table 4
Single Targets Previously Searched for Multiplicity

Object Name	RA (2000)	Dec (2000)	Reference
WSB 16/DoAr 15[1]	16 23 34.7	-23 40 29.0	A97
V852 Oph	16 25 22.16	-24 30 13.7	This work
IRS 9	16 25 49.07	-24 31 38.8	C00
ROXs 3	16 25 49.65	-24 51 31.7	S95
ROXs 4/IRS10	16 25 50.53	-24 39 14.3	This work
ROXs 6/SR 4	16 25 56.18	-24 20 48.2	G93;S95;C00
ROXs 7/IRS 13/GSS20[2]	16 25 57.54	-24 30 31.7	A97; C00; IRS11 is 25.705″away
ROXs 8/DoAr 21/GSS23	16 26 03.05	-24 23 01.63	G93;S95;A97;C00
GSS25/SR 3	16 26 09.33	-24 34 12.1	S95; C00
GSS26	16 26 10.35	-24 20 54.7	C00
GSS29	16 26 16.87	-24 22 23.0	S95
ROXs 10A/DoAr24	16 26 17.09	-24 20 21.4	G93;This work
VSSG1/Elias 20	16 26 18.89	-24 28 19.6	C00
GSS30 IRS1/Elias 21[3]	16 26 21.42	-24 23 02.3	C00
DoAr25/GY17	16 26 23.69	-24 43 14.0	C00
ROXs 9A	16 26 23.99	-25 47 16.1	This work
Elias 24/WSB 31	16 26 24.09	-24 16 13.3	C00
ROXs 9B	16 26 30.72	-25 43 39.8	This work
ROXs 9C	16 26 37.95	-25 45 12.8	This work
WSB 37/GY93	16 26 41.28	-24 40 17.8	C00
WL16	16 27 02.35	-24 37 27.2	S95; C00
WL15/Elias 29	16 27 09.44	-24 37 18.7	S95; C00
GY224	16 27 11.20	-24 40 46.6	HBGR02
WL19	16 27 11.73	-24 38 31.9	HBGR02
WL4	16 27 18.50	-24 29 05.9	C00
VSSG 22	16 27 22.92	-24 17 57.3	C00
IRS 48	16 27 37.18	-24 30 35.2	S95; C00
IRS32b/GY235[4]	16 27 13.84	-24 43 31.6	S95
GY292	16 27 33.11	-24 41 15.1	This work
IRS 50	16 27 38.12	-24 30 43.1	C00
ROXs 35A	16 27 38.31	-23 57 32.9	This work
IRS 49	16 27 38.31	-24 36 58.7	S95; C00
WSB 52/GY314	16 27 39.43	-24 39 15.5	S95, This work
IRS 51	16 27 39.83	-24 43 14.9	S95;C00; HBGR02
IRS 56	16 27 50.72	-24 48 21.4	S95
IRS 54	16 27 51.79	-24 31 45.7	C00
SR 10	16 27 55.56	-24 26 18.1	S95; C00
WSB 60	16 28 16.51	-24 36 58.0	S95; C00
WSB 63	16 28 54.09	-24 47 44.2	S95
WSB 67[5]	16 30 23.31	-24 54 16.2	S95
ROXs 39[1]	16 30 35.6	-24 34 15.0	A97
ROXs 40	16 30 51.51	-24 11 34.0	This work
WSB 69A	16 31 04.37	-24 04 33.3	This work
WSB 69B	16 31 05.17	-24 04 40.3	This work
ROXs 44/Haro1-16	16 31 33.45	-24 27 37.1	S95;This work
IRS 63	16 31 35.67	-24 01 29.3	HBGR02
IRAS 16289-2457	16 31 54.74	-25 03 23.8	This work
IRS 67	16 32 01.01	-24 56 41.9	HBGR02

[1] Coordinates from SIMBAD database

[2] WSB 16 is associated with extended optical nebulosity (Ageorges et al. 1997)

[3] GSS30 IRS1 coordinates are from Zhang et al. (1997)

[4] Verification of association membership remains to be established (Simon et al. 1995)

[5] Coordinates for WSB 67 are precessed from Simon et al. (1995)